AIP | Journal of Applied Physics

Carrier transfer and redistribution dynamics in vertically aligned stacked In0.5Ga0.5As quantum dots with different GaAs spacer thicknesses

Ho-Sang Kwack, Yong-Hoon Cho, Jin-Dong Song, Won-Jun Choi, and Jung-Il Lee

Citation: J. Appl. Phys. **106**, 123524 (2009); doi: 10.1063/1.3272712
View online: http://dx.doi.org/10.1063/1.3272712
View Table of Contents: http://jap.aip.org/resource/1/JAPIAU/v106/i12
Published by the American Institute of Physics.

Carrier transfer and redistribution dynamics in vertically aligned stacked $In_{0.5}Ga_{0.5}As$ quantum dots with different GaAs spacer thicknesses

Ho-Sang Kwack,[1] Yong-Hoon Cho,[1,a)] Jin-Dong Song,[2] Won-Jun Choi,[2] and Jung-Il Lee[2]
[1]*Department of Physics, Graduate School of Nanoscience and Technology (WCU) and KI for the NanoCentury, KAIST, Daejeon 305-701, Republic of Korea*
[2]*Nano Device Research Center, Korea Institute of Science and Technology, Seoul 136-791, Republic of Korea*

(Received 5 July 2009; accepted 11 November 2009; published online 28 December 2009)

We have investigated optical and structural properties of three-stacked InGaAs quantum dot (QD) structure with GaAs spacer thicknesses of 22, 35, and 88 nm (denoted by QD22, QD35, and QD88, respectively) grown by migration-enhanced molecular beam epitaxy. From temperature-dependent photoluminescence (PL) analysis, it is found that thermal carrier redistribution between vertically adjacent QD layers plays an important role as the thickness of GaAs spacer is reduced from 88 to 22 nm. Although the QD sizes of upper layers are quite similar to those of the first bottom layer, the QDs of the upper layers appear to emit at higher energies probably due to different alloy compositions caused by the strain-induced intermixing effect between InGaAs QDs and GaAs barriers with stacking. Especially for QD22 sample, we observed thermally assisted carriers transfer among vertically adjacent QD layers with increasing temperature by using time-resolved PL measurements, which is in good agreement with the temperature dependence of integrated PL intensity and peak energy position. © *2009 American Institute of Physics*. [doi:10.1063/1.3272712]

I. INTRODUCTION

In recent years, a lot of research efforts have been devoted to In(Ga)As/GaAs quantum dots (QDs) due to their great potential for optoelectronic devices such as semiconductor lasers,[1] semiconductor optical amplifiers,[2] QD microcavity light-emitting-diodes,[3] and QD infrared photodetectors[4] for its use in fiber optic communications. The studies of various QD structures have permitted the identification of unique and interesting physical phenomena such as low threshold current density, high characteristic temperature, and high differential gain in laser diodes.[5,6] For many practical purposes, the precise control of QD shape and size distribution in QD growth as well as the understanding of carrier dynamics between QD layers are expected to play an important role in practical device applications. In particular, injected carriers into QD devices populate in the continuum states such as barriers and/or wetting layers (WLs) and then these carriers transfer into lower energy levels via various processes including carrier capture processes into excited states (ESs) and/or ground state (GS) of QDs before radiative recombination. These carrier relaxation and recombination processes will affect the quantum efficiency of carriers captured in the states of QDs.[7,8] In our previous studies, we have reported the QD shape and size distribution with variation in the number of stacking layers.[9] The QDs grown by migration-enhanced molecular-beam epitaxy (MEMBE), also known as atomic layer molecular-beam epitaxy, have been studied with a view to solving the uniformity problems[10,11] as well as to expecting the weaker WL effect.[12] Based on the previous studies, the inhomogeneous broadening due to vertically stacked QD size variation could be carefully controlled by GaAs spacer thickness during QD growth, which will be useful for broad-band QD applications such as semiconductor optical amplifiers or multicolor QD infrared detectors.

In this work, the carrier dynamics and the optical properties of three-stacked $In_{0.5}Ga_{0.5}As$ QD layers with different spacer thicknesses grown by MEMBE are systemically investigated by transmission electron microscopy (TEM), low-power-excitation photoluminescence (PL), excitation-power- and temperature-dependent PL, and time-resolved PL (TRPL) techniques. From these results, we investigate the different origins and carrier dynamics of distinctive double peaks observed from the three-stacked InGaAs QD samples with different GaAs spacer thicknesses.

II. EXPERIMENT

$In_{0.5}Ga_{0.5}As/GaAs$ QDs used in the present work were grown on semi-insulating GaAs substrates by MEMBE method. After deposition of a 50-nm-thick $Al_{0.3}Ga_{0.7}As$ layer, 20 pairs of short period superlattices (SLs) consisting of a 2-nm-thick $Al_{0.3}Ga_{0.7}As$ layer and a 2-nm-thick GaAs layer were sequentially deposited at the growth temperature (T_g) of 570 °C. A series of samples of three-stacked QD layers with GaAs spacer thicknesses of 22, 35, and 88 nm was prepared, which will be denoted by QD22, QD35, and QD88, respectively. Each QD layer was grown by five repeated deposition of 1-ML-thick InAs and 1-ML-thick GaAs at T_g=510 °C. Growth interruptions were used during every interval between deposition of indium and exposure to arsenic. Then, 20 pairs of short period SLs consisting of a 2-nm-thick $Al_{0.3}Ga_{0.7}As$ layer and a 2-nm-thick GaAs layer were deposited again, and finally capped by a 10-nm-thick $Al_{0.3}Ga_{0.7}As$ layer and a 4-nm-thick GaAs layer. For com-

a)Electronic mail: yhc@kaist.ac.kr.

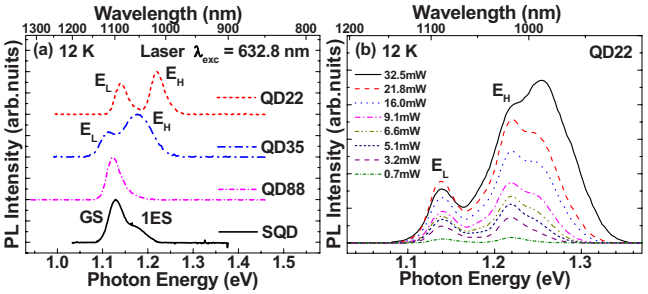

FIG. 1. (Color online) (a) 12 K PL spectra of QD22, QD35, QD88, and SQD samples were taken by using a cw He–Ne laser ($P_{exe} \sim 0.7$ mW). The curves are vertically shifted for clarity. (b) Excitation power-dependent PL spectra of three-stacked InGaAs QD layer with GaAs spacer thicknesses of 22 nm in the excitation power range from 0.7 to 32.5 mW.

parison, we also prepared a control sample containing a single stack of $In_{0.5}Ga_{0.5}As$ QDs, which will be denoted by SQD. The averaged QD density, width, and height in SQD were estimated to be about 1.5×10^{10} cm^{-2}, ~45 nm, and ~6.2 nm by using atomic force microscopy, respectively.[10] PL experiments were carried out as a function of temperature ranging from 17 to 300 K using the 632.8 line of a cw He–Ne laser. Excitation power-dependent PL measurements were performed at low temperature to confirm the position of the excited states of $In_{0.5}Ga_{0.5}As$ QDs wherein the excitation power was varied from 0.7 to 32.5 mW. A mode-locked, fs pulsed Ti:sapphire laser was used for TRPL as an excitation light source with the instrument response function (IRF) of ~30 ps. The signal was detected using a microchannel plate photomultiplier tube and the time-correlated signal was analyzed with a time-correlated single photon counting system.

III. RESULTS AND DISCUSSIONS

Figure 1(a) shows 12 K PL spectra of three-stacked $In_{0.5}Ga_{0.5}As$ QD samples with different GaAs spacer thicknesses (QD22, QD35, and QD88) and SQD sample. For SQD sample, we observed a main emission peak at 1.126 eV originated from the GS with a higher energy side shoulder at 1.182 eV corresponding to the first ES. On the other hand, we observed that two separated peaks centered at 1.117 (1.140) and 1.169 eV (1.221 eV) for QD35 (QD22) sample, respectively. As the thickness of GaAs spacer is reduced from 88 to 22 nm, an additional strong peak appears at the high-energy side (E_H) of the spectrum, whereas the position and the width of the low-energy side (E_L) emissions are nearly the same. Figure 1(b) shows the excitation-power-dependent PL spectra measured at 12 K for QD22 sample with an increase in the excitation power ranging from 0.7 to 32.5 mW. The PL intensities of both E_L and E_H peaks increase linearly and their relative intensities were kept constant at the excitation power ranging from 0.7 to ~20 mW. We have also performed low-power-excitation PL by using the quasimonochromatic light from a 250 W halogen lamp dispersed by a monochromator,[9] so the contribution of excited states of QDs to these PL spectra may be negligible. In spite of the very low excitation power, we observed that E_H peak of the QD emission appears strongly for both QD22 and QD35 samples. In addition, the energy separation (ΔE)

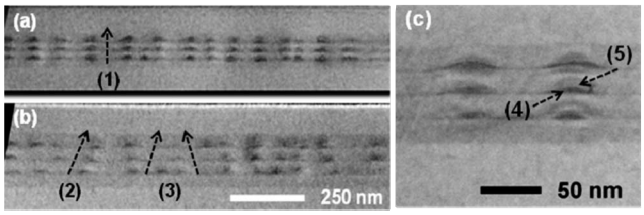

FIG. 2. Cross-sectional TEM images of three-stacked (a) QD22 and (b) QD35 samples with different spacer thicknesses, respectively. (c) Enlarged view of TEM image for QD22 sample.

between E_L and E_H peaks becomes larger with decreasing GaAs spacer thickness, as seen in Fig. 1(a). For instance, ΔE is 81 meV for QD22 sample, which is much larger than that of between GS and ES (~56 meV) in SQD sample. It has been reported that ΔE between GS and ES for In(Ga)As QDs with different capping layers varies in the range of about 54–58 meV,[4] which is in good agreement with the results of SQD sample. These results indicate that the origins of both E_L and E_H peaks in QD22 sample are attributed to two types of QDs with different sizes and/or alloy composition distributions in the QD ensemble.[13] The PL spectra of QD88 sample measured with an increase in excitation power are very similar to those of SQD sample,[9] and the ΔE values between GS and ES in QD88 and SQD samples are almost the same (~56 meV). Therefore, the peaks of PL spectra for QD88 sample are attributed to the transitions of GS and ES, indicating no electrical coupling between three-stacked QDs with 88 nm GaAs spacer layers.

In order to understand the difference in the optical properties and to investigate the structural properties of QD22 and QD35 samples, TEM experiments were performed. Figure 2 shows the cross-sectional TEM images of (a) QD22 and (b) QD35 samples, respectively. To obtain the distinct TEM images, the samples were carefully prepared by using the focused ion beam milling technique instead of conventional ion milling technique. The QDs in the upper layers are vertically aligned well along the growth direction (indicated by arrow 1) for QD22 sample [Fig. 2(a)], while those are weakly aligned to the QDs in the first bottom layer (indicated by arrow 2) and show complex QD size distribution for QD35 sample [Fig. 2(b)]. It is found that upper QDs grown on closely spaced two QDs in the first bottom layer get merged into one with an increase in the number of stacks of QD layers (indicated by arrow 3), probably due to the strain fields along the vertical direction from the first layer of GaAs spacer[14,15] Therefore, we can anticipate that the larger broadening of the E_H peak at the QD35 sample in Fig. 1(a) as compared to that at the QD22 sample is due to the mixture of emissions caused by variation in the QD size and/or alloy composition distribution at different stacks.[16] Although the sizes of upper QDs are quite similar to (or slightly larger than) those of bottom QDs for QD22 sample [Fig. 2(c)], the emission of upper QD layers appears to emit at higher energies, as shown in Fig. 1(a), probably due to alloy composition differences. In general, an increased size of QDs with stacking is due to the effect of elastic strain relaxation caused by penetrating strain fields, resulting in an energy redshift of the PL spectrum. However, we observed the high-contrast

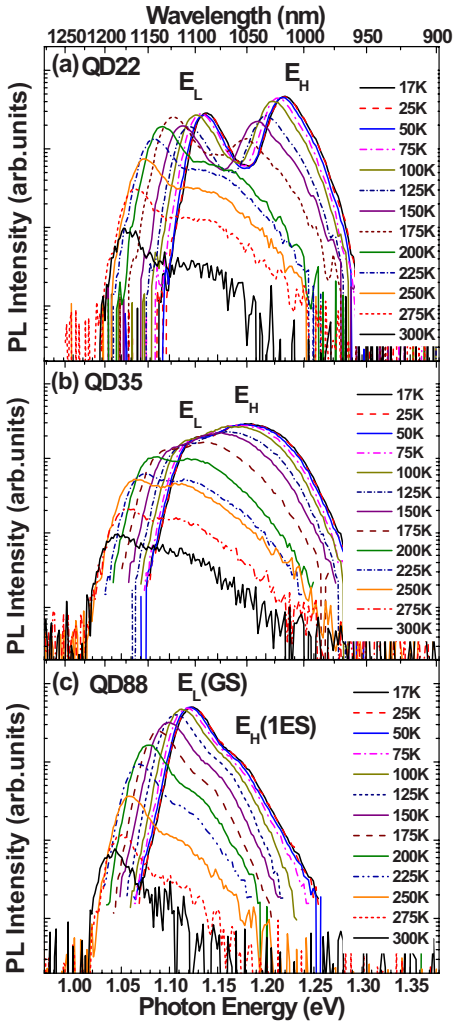

FIG. 3. (Color online) Temperature-dependent PL spectra for (a) QD22, (b) QD35, and (c) QD88 samples in the temperature range from 17 to 300 K, respectively.

QDs (indicated by arrow 4) and low-contrast QDs (indicated by arrow 5) in the same QD for QD22 sample from enlarged view of TEM image, as seen in Fig. 2(c). These contrast differences at the same InGaAs QDs may reflect alloy composition differences caused by the strain-induced material intermixing effect between InGaAs QDs and GaAs barriers. Based on the PL and TEM results, we conclude that the E_L peaks of QD22 and QD35 samples originate from the GS emission in the first bottom QDs layer as these spectral features are similar to those of QD88 and SQD samples with no electrical coupling between stacks, while the E_H peaks of QD22 and QD35 samples originate primarily from the GS emission in the second and/or the third QDs layers.

Figure 3 shows temperature-dependent PL spectra of QD22, QD35, and QD88 samples measured in the temperature range varying from 17 to 300 K with an excitation power of ~0.7 mW. Although the whole PL intensities gradually decrease with increasing temperature, PL intensities of E_H peak decrease faster than those of E_L peak for all the QD samples. This behavior can be attributed to rapid thermal escape of carriers confined in higher ES or in QDs with higher band-gap energy with increasing temperature. Two peaks in each PL spectrum are separated by Gaussian multipeak fitting method, so we could obtain PL peak energies and PL intensities of E_L and E_H peaks with temperature, as seen in Fig. 4. The integrated PL intensities of E_L and E_H peaks for the QD88 sample gradually decrease with increasing temperature caused by the thermal escape of carriers [Fig. 4(b)], while those for the QD22 sample [Fig. 4(a)] are quite different from those of the QD88 sample. The PL intensities of E_L peak for the QD22 sample were kept constant in the temperature range from 17 to 100 K, decreases slightly until 150 K, increases up to 175 K, and then finally decreases again until 300 K. This behavior can be attributed to the carrier transfer among vertically three-staked QD layers, since the lateral QD coupling seems smaller due to larger separation between adjacent QDs in lateral direction as seen in Fig. 2.[14] Figure 4(c) depicts the integrated PL intensities for the QD22, QD35, QD88, and SQD samples as a function of temperature, which are normalized for comparison. We observed that the integrated PL intensities for the QD88 and SQD samples decrease continuously with increasing temperature, while those for the QD22 and QD35 samples remain nearly constant between 125 and ~175 K. Temperature dependence of the integrated PL intensity for QD35 sample shows intermediate behavior between those of QD22 and QD88 samples, since the GaAs spacer layer thickness (~35 nm) is near at the boundary for the strain field penetration, as seen in Fig. 2(b). Figure 4(d) shows the peak energy positions of E_L and E_H peaks for the QD22, QD35, and QD88 samples measured as a function of temperature. The temperature dependence of QD emission peak energy position $E(T)$ can be expressed by Varshni's equation $E(T) = E(0) - \alpha T^2/(\beta + T)$, where the parameters α and β are determined by fitting the experimental data. We fitted all $E(T)$ data to Varshni's equation with $\alpha = 5.1 \times 10^{-4}$ eV/K and $\beta = 250$ K (curves V1–V5) obtained from the SQD data. For QD88 sample, $E(T)$'s for GS peak (open triangle) and ES peak (closed triangle) fit well with the curves V5 and V3, respectively. For the QD22 and QD35 samples, $E(T)$'s for each E_L peak (open circles and open squares) fit well with the curves V4 and V5, while $E(T)$'s for each E_H peak (closed circle and closed square) do not fit well with the calculated curves V1 and V2, respectively. At 125–150 K, $E(T)$'s for E_H peaks of QD22 and QD35 samples start to deviate from the calculated curves V1 and V2, respectively. At 150–200 K, the $E(T)$ values for E_H peaks of the QD22 and QD35 samples become dramatically reduced, and then ΔE's of the QD22 and QD35 samples follow well that of QD88, even though the E_L peak position is slightly varied between samples. Therefore, the observed optical features of E_H peaks at both QD22 and QD35 samples with increasing temperature can be attributed to GS emissions of E_H peak for $T < 125$ K, the mixture of emissions between GS of E_H peak and ES of E_L peak for 125 K $< T <$ 200 K, and ES of E_L peak for $T > 200$ K.

To elucidate the carrier dynamics of three-stacked InGaAs QDs samples, TRPL measurements were carried out at 17 K with an excitation wavelength of 800 nm and a power of 4 μJ/cm^2. Figure 5 shows measured rise time (τ_R) and decay time (τ_D) of both (a) QD22 and (b) QD88 samples as a function of the detection wavelength in the entire PL band.

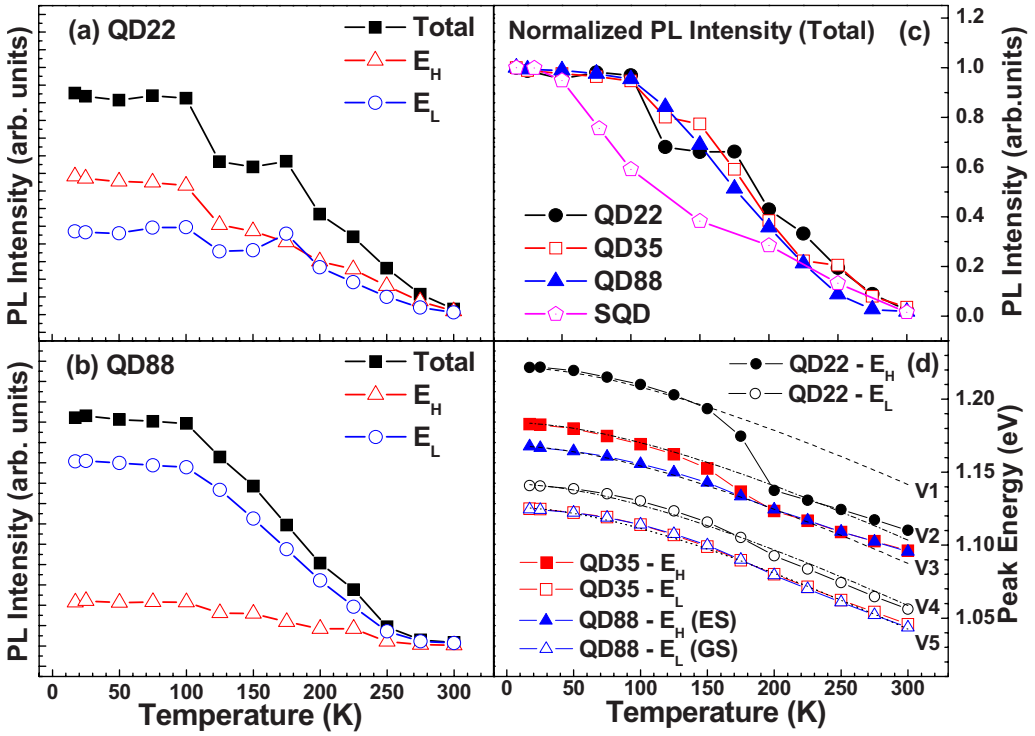

FIG. 4. (Color online) The integrated PL intensities of the whole PL spectra and each of deconvoluted peak (E_L and E_H peaks) from the PL spectra of (a) QD22 and (b) QD88 samples, respectively. (c) Spectrally integrated PL intensities and (d) PL peak positions for three-stacked InGaAs QDs with different GaAs spacer thicknesses as a function of temperature.

The τ_R difference ($\Delta\tau_R$) between E_L and E_H peaks of QD22 sample was estimated to be ~21 ps, while $\Delta\tau_R$ of QD88 sample is ~86 ps (i.e., the relaxation time from ES to GS in this case) as a function of detection energy. These results indicate that the filling of E_L and E_L states in QD22 sample is due to carrier relaxation from continuum state (barrier or WL), while the filling of E_L state (GS) in QD88 sample is mainly due to carrier relaxation from E_H state (ES). The large value of $\Delta\tau_R$ (~86 ps) of QD88 sample reflects the existence of phonon bottleneck in our sample since the ΔE (~56 meV) between ES and GS is larger than the optical phonon energy in the In(Ga)As QDs (30–36 meV).[16,17] For QD22 sample [Fig. 5(a)], τ_D in the entire PL band of E_L-peak was kept constant, while τ_D in the entire PL band of E_H peak slightly reduces with increasing detection energy. This suggested that the carriers at GS in the same layer are spatially separated well, which is similar to that of QD88 sample in Fig. 5(b). In order to explain these behaviors at QD ensemble, many groups have been frequently used a suggesting lateral coupling through interdot tunneling.[18,19] For our samples, however, this model is not suitable due to the difficulty of lateral coupling between adjacent QDs, as seen in Fig. 2(a). From the TEM results, the average separation for QD22 sample between adjacent QDs in the last top layer is observed to be ~40 nm, whereas the upper layers of QDs are well aligned along the QDs in the first bottom layer (E_L peak). Therefore, τ_D at E_H peak of QD22 sample can be attributed to either the electrical coupling between vertically adjacent QDs or the confining potential-dependent exciton oscillator strength (F_e).[20] However, we can rule out the effect of F_e because the average size of our QD sample is about 45 nm, which is larger than the 37 nm Bohr radius in InAs material.[21]

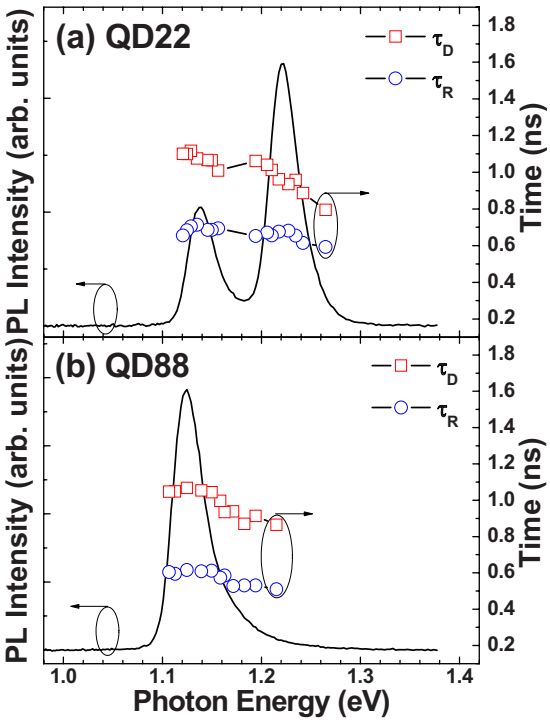

FIG. 5. (Color online) Rise times (open circle) and decay times (open square) of (a) QD22 and (b) QD88 samples as a function of the detection wavelength in the entire PL band. 17 K PL spectra are plotted together for comparison, respectively.

Figure 6 depicts τ_D as a function of temperature for (a) E_L and (b) E_H peaks of all the three-stacked InGaAs QDs

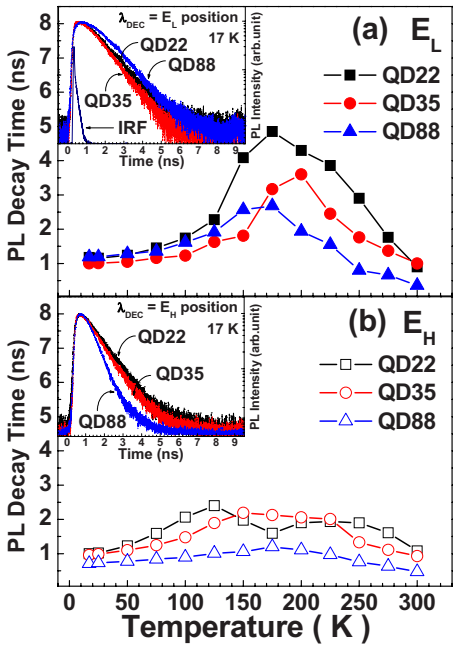

FIG. 6. (Color online) Decay times at (a) E_L peak and (b) E_H peak for all samples are depicted with increasing temperature. The inset shows the normalized TRPL spectra of (a) E_L peak and (b) E_H peak at 17 K.

samples. The inset shows a logarithmic scale plot of the normalized TRPL related to (a) E_L and (b) E_H peaks for all samples at 17 K, respectively. A monoexponential decay profile was seen for QD22, QD35, and QD88 emissions. By fitting of monoexponential functions $I(t)=A_1 \exp(-t/\tau_D)$, τ_D for E_L peak of all samples were extracted out to be ~1.1 ns (QD22), ~1.0 ns (QD35), and ~1.1 ns (QD88) (with an IRF of ~30 ps). The measured τ_D of photoexcited carriers can be governed by two competing processes. One is the radiative process which mainly depends on wave-function overlap which is influenced by QD size, shape, and height of its localizing potential. The other is the nonradiative process including multiphonon emission, trap at defects, recombination at impurities, and so on. For QD22, QD33, and QD88 samples in Fig. 6(a), the increase in τ_D with varying temperature from 17 to 175 K is indicative of dominant radiative recombination process due to the effective carrier localization in QDs, while the decrease in τ_D with increasing temperature further above 175 K indicates the increasing influence of nonradiative recombination centers with temperature. For QD22 sample, τ_D of E_L peak begins to increase rapidly at 125 K [Fig. 6(a)], while τ_D of E_H peak begins to decrease slightly at the same temperature [Fig. 6(b)]. Moreover, we did not see this phenomenon (slow-fast-slow) at τ_D of E_H peak (open triangle) for the QD88 sample [Fig. 6(b)] because there is no electrical coupling between three-stacked QDs with 88 nm GaAs spacer layers. Therefore, the temperature dependence of τ_D for E_L and E_H peaks in the QD22 sample at 125 K$<T<$175 K can be explained by the thermal carrier redistribution from the upper QD layers (E_H peak) to the first QD layer (E_L peak) with increasing temperature. This is also in good agreement with the temperature dependence of integrated PL intensity [Fig. 4(a)] and the peak energy position [Fig. 4(d)]. We observed that τ_D of E_H peak increases again at ~200 K for QD22 sample in Fig. 6(b), which can be attributed to a predominant ES emission of E_L peak compared to GS emission of E_H peak for $T>200$ K [Figs. 3(a) and 4(d)]. It is interesting to note that for $T>200$ K, the τ_D values of E_L and E_H peaks (which correspond to GS and ES emissions in QD22 sample, respectively) are larger than those in the QD88 sample, reflecting that the carriers of the upper QD layers transfer into the GS or ES levels of E_L peak with increasing temperature via the thermal carrier redistribution.

IV. CONCLUSIONS

For three-stacked $In_{0.5}Ga_{0.5}As$ QDs with the thicknesses of GaAs spacer of 22, 35, and 88 nm grown by MEMBE, the position and the width of the emission at the E_H peak position are changed, whereas those of the emission at the E_L peak position are nearly unchanged. From the excitation power- and temperature-dependence PL, and TEM analysis, we found that well-separated two emissions originate from vertically aligned InGaAs QD layers with different alloy compositions caused by the effect of strain-induced intermixing with stacking. Temperature dependence of the integrated PL intensity for QD35 sample shows intermediate behavior between those of QD22 and QD88 samples, since the GaAs spacer layer thickness (~35 nm) is near at the boundary for the strain field penetration. In particular, for QD22 sample, we note that the carriers transfer from upper layers to the first bottom layer with elevating temperature via the thermal carrier redistribution between vertically adjacent QD layers. These behaviors can help to improve understanding of the dependence of the optical properties on the GaAs spacer thickness during MEMBE growth, which will provide advice in further design optimization of the multilayer QD structures for optoelectronic device applications.

ACKNOWLEDGMENTS

This work was supported by the NRL Program (Grant No. R0A-2005-000-10130-0), the Nano R&D Program (Grant No. 2008-02981), and the WCU Program (Grant No. R31-2008-000-10071-0) funded by the Ministry of Education, Science and Technology.

[1] S. M. Kim, Y. Wang, M. Keever, and J. S. Harris, IEEE Photonics Technol. Lett. **16**, 377 (2004).
[2] H. Su and S. L. Chuang, Appl. Phys. Lett. **88**, 061102 (2006).
[3] Z. Y. Zhang, Z. G. Wang, B. Xu, P. Jin, Z. Z. Sun, and F. Q. Liu, IEEE Photonics Technol. Lett. **16**, 27 (2004).
[4] E. T. Kim, Z. Chen, and A. Madhukar, Appl. Phys. Lett. **81**, 3473 (2002).
[5] X. Huang, A. Stintz, H. Li, L. F. Lester, J. Cheng, and K. J. Malloy, Appl. Phys. Lett. **78**, 2825 (2001).
[6] H. Y. Liu, D. T. Childs, T. J. Badcock, K. M. Groom, I. R. Sellers, M. Hopkinson, R. A. Hogg, D. J. Robbins, D. J. Mowbray, and M. S. Skolnick, IEEE Photonics Technol. Lett. **17**, 1139 (2005).
[7] J. Siegert, S. Marcinkevicius, K. Fu, and C. Jagadish, Nanotechnology **17**, 5373 (2006).
[8] M. Gurioli, A. Vinattieri, M. Zamfirescu, M. Colocci, S. Sanguinetti, and R. Nötzel, Phys. Rev. B **73**, 085302 (2006).
[9] H. S. Kwack, B. O. Kim, Y. H. Cho, J. D. Song, W. J. Choi, and J. I. Lee, Nanotechnology **18**, 315401 (2007).
[10] J. D. Song, Y. J. Park, I. K. Han, W. J. Choi, W. J. Cho, J. I. Lee, Y. H. Cho, and J. Y. Lee, Physica E , **26**, 86 (2005).

[11]J. D. Song, Y. M. Park, J. C. Shin, J. G. Lim, Y. J. Park, W. J. Choi, I. K. Han, J. I. Lee, H. S. Kim, and C. G. Park, J. Appl. Phys. **96**, 4122 (2004).
[12]N. K. Cho, S. P. Ryu, J. D. Song, W. J. Choi, J. I. Lee, and H. Jeon, Appl. Phys. Lett. **88**, 133104 (2006).
[13]M. O. Lipinski, H. Schuler, O. G. Schmidt, K. Eberl, and N. Y. Jin-Phillipp, Appl. Phys. Lett. **77**, 1789 (2000).
[14]Q. Xie, A. Madhukar, P. Chen, and N. P. Kobayashi, Phys. Rev. Lett. **75**, 2542 (1995).
[15]X. D. Wang, N. Liu, C. K. Shih, S. Govindaraju, and A. L. Holmes, Appl. Phys. Lett. **85**, 1356 (2004).
[16]R. Heitz, H. Born, F. Guffarth, O. Stier, A. Schliwa, A. Hoffmann, and D. Bimberg, Phys. Rev. B **64**, 241305 (2001).
[17]P. Bhattacharya, S. Ghosh, and A. D. Stiff-Roberts, Annu. Rev. Mater. Res. **34**, 1 (2004).
[18]Yu. I. Mazur, J. W. Tomm, V. Petrov, G. G. Tarasov, H. Kissel, C. Walther, Z. Ya. Zhuchenko, and W. T. Masselink, Appl. Phys. Lett. **78**, 3214 (2001).
[19]H. Kissel, U. Muller, C. Walther, T. Masselink, Y. I. Mazur, G. G. Tarasov, and M. P. Lisitsa, Phys. Rev. B **62**, 7213 (2000).
[20]Y. C. Zhang, A. Pancholi, and V. G. Stoleru, Appl. Phys. Lett. **90**, 183104 (2007).
[21]H. Fu, L. W. Wang, and A. Zunger, Phys. Rev. B **59**, 5568 (1999).